ISSN:1991-8178

Australian Journal of Basic and Applied Sciences

Journal home page: www.ajbasweb.com

Superconducting Properties of $Bi_{1.7}$ $Pb_{0.3}$ $Sr_2Ca_2Cu_3$ $O_{10+\delta}$ Added with Nano Particle γ Al_20_3.

Bushra A. Aljurani and Khalid A. Shyaa

University of Baghdad, Collage of science, Department of physics, Baghdad Iraq

ARTICLE INFO

Article history:
Received 10 October 2015
Accepted 30 November 2015
Available online 24 December 2015

Keywords:
Bi-based superconductors, γ (Al_2O_3) nano addition, Scanning electron microscope.

ABSTRACT

γAl_2 O_3 nano powders with average size 50 nm were introduced into γ (Al_2 O_3) ($Bi_{1.7}$ $Pb_{0.3}$ Ca_2 Cu_3 $O_{10+\delta}$) with (x=0.0, 0.2, 0.4, 0.6, 0.8, and 1) wt. % in the pellet form. The samples were prepared by solid state reaction method. γ Al_2O_3 nano particles were added to the BSCCO system in order to improve the connectivity among the grains will leading to increase the critical temperature and volume fraction of high T_c phase. XRD analysis showed that both (Bi, Pb)-2223 and Bi-2212 phases coexist in the sample were having orthorhombic crystal structure. The SEM images of the fractured surface of the superconducting samples as plate-like structure. The highest critical temperature is 118K for x=0.2 wt. %. The nanoparticle with size closer to the coherence length was more effective in enhancing T_c.

© 2015 AENSI Publisher All rights reserved.

ToCite ThisArticle: Bushra A. Aljurani and Khalid A. Shyaa., Superconducting Properties of $Bi_{1.7}$ $Pb_{0.3}$ $Sr_2Ca_2Cu_3$ $O_{10+\delta}$ Added with Nano Particle γ AI_20_3.***Aust. J. Basic & Appl. Sci.,*** *9(35): 54-60, 2015*

INTRODUCTION

The field of superconductivity undergoes a major turnaround in 1986 following the discovery of high temperature superconductivity (HTS) in the copper oxide based materials which were later found to superconduct above the boiling point of liquid nitrogen (Abd Shukor, R., 2004). After the discovery of Bi-based superconducting systems, a great amount of work concerning preparation, superconducting properties, and the structure of these compounds has been done (Maeda, H., 1988; Michel, C., 1987). Many researchers have investigated the effects of oxides substitution or addition on the superconducting and structural properties of BSCCO system and they found that. The enhancement or destruction of the superconducting properties depends on the characteristics of the dopant material nature and the substitution site. (Yildirim, S., 2012; Rentschler, T., 1992), the works of these researches are related to addition or substitution of micro-oxide powders to BSCCO systems. With nano technology developments a wide range of nanostructure materials has been synthesized. When nanoparticles are added to the BSCCO system, due to the tiny size of nanoparticles, they settle easier and much more among the grains of these ceramic superconductors than the micro size dopant. If adequate amount of nanoparticles with metallic character is added to the BSCCO, the inter grain connectivity will possibly improve. The effect of nano-size TiO_2 addition on the microstructure on the pinning properties of polycrystalline (Bi, Pb)-2223 were studied by Hamid (2009). The TiO_2 content in the sample varied from 0.05 to 0.1 wt. % of the total mass of the sample. They found that J_c, T_c andC-axis parameter decreases with the addition of TiO_2.

Bi-2223 superconductor system was prepared by solid state reaction technique with intermediate grinding by added with nano particle of Sm_2O_3 with x = 0.0, 0.05 wt. %. They found that addition of Sm_2O_3 nano particle slowly decreased the volume fraction of Bi-2223 phase and accelerated the formation of the Bi-2212 phase for x = 0.0, 0.02 samples. Changes in superconducting properties of Sm-added Bi-2223system were discussed by Baqiah (2009).

The effect of different nano sized CO_3O_4 (10, 30, and 50 nm) addition on the $Bi_{1.6}Pb_{0.4}Sr_2Ca_2$ Cu_3O_{10} $(Co_3O_4)_x$ superconductor with x=0.0, 0.05 wt. % were investigated by Jannah (2013). The samples were prepared by the solid state reaction method. They found that samples with x= 0.01 wt. %. Co_3O_4 (10 nm) showed the highest T_c at 102 K. The X-ray diffraction patterns of all the samples indicated the majority Bi-2223 phase along with minor Bi-2212 and Bi-2201 phases. The sample with x=0.01 wt. % of the added Co_3O_4 (10, 30) nm size showed the highest volume fraction of Bi-2223 phase (72 %) and the highest superconducting transition temperature.

Corresponding Author: Bushra A. Aljurani, University of Baghdad, Collage of science, Department of physics, Baghdad Iraq

In this paper the nanoparticleγ Al_2O_3 with average size (50) nm were added to the Bi, Pb-Sr-Ca-Cu system to improve the connectivity between grains. The physical properties such as electrical, structural and morphological properties of the γ $(Al_2O_3)_x(Bi_{1.7}Pb_{0.3}Sr_2Ca_2\ Cu_3O_{10+\delta})$ with (x=0.00, 0.2, 0.4, 0.6, 0.8, and 1) wt.% were investigated XRD, SEM, and AFM were used for morphological and structural characterization of the prepared samples. DC resistivity measurement was formed to study the superconducting properties of the samples and to achieve the optimum amount of γAl_2O_3 nanoparticle addition to the BSCCO system investigated. The BSCCO samples were prepared by solid state reaction technique that obtain a high T_c.

Experimental Details:

γ $(Al_2O_3))(Bi_{1.7}\ Pb_{0.3}\ Sr_2\ Ca_2\ Cu_3\ O_{10+\delta})$ with x=0.0 0.2, 0.4, 0.6, 0.8, and 1)wt.% prepared by conventional solid-state reaction method. Appropriate amounts of Bi_2O_3 (99.9%) PbO (99.9%), $Sr(NO_3)_2$ (99.9%), CaO (99.9%), CuO (99.9%), and Al_2O_3 (99.9%), powders were used as starting materials. The powder of precursor was mixed together by using agate mortar. The mixture homogenization takes place by adding a sufficient quantity of 2-propanol to form a past during the process of grinding from about (1h). In the second step, the materials were grounded to a fine powder and then calcined in air at 800^{o}C for (24) h, the mixture was then pressed into pellets (1.3 cm) in diameter and (0.2 cm) thick, using hydraulic type (SPECAC), under pressure of o.7 GPa. The pellets were sintered in air at 830^{o}C for 140 h. Four probe dc method at temperature range (77-300) K was used to measure the resistivity (ρ) and to determine the critical temperature (T_c) of the sample. The X-ray powder diffraction pattern for each sample was obtained using Cu Kα (1.54 ^{o} A) radiation in the range 2θ = 5-60^{o}using X-ray diffract meter type Philips which has the following features: Source: Cu $_{K\alpha}$, wavelength (λ): 1.5405^{o}A, Current: 20 mA, 2θ range: 20 – 60 degrees, Voltage: 40 kV, scanning speed: 0.1 degrees/min. Phase purity and the lattice parameters were obtained from these patterns. SEM and AFM imaging were used to examine the surface morphology and grain structure of the samples and EDS was applied for the elemental analysis of the samples. SEM images was taken by using VEGA\\TESCAN-SEM (SEM Hv 30.00 kV). Scanning Electron Microscope. AFM images was taken by using (Scanning probe Microscope type AA3000), Atomic Force Microscope.

RESULTS AND DISCUSSION

EDX Analyses:

The quantitative values of the atomic compositions presenting in the $(Al_2O_3)_xBi_{1.7}Pb_{0.3}Sr_2Ca_2Cu_3O_{10+\delta}$ grains of samples with x=0.0 and 0.6 wt. % are analytically investigated by the Energy Dispersive X-ray Spectroscope (EDX) and shown in Figs.(1 a & b). The Fig. (1), shows Bi, Sr, Ca, Cu, and O element composition mapping taken on the surface of the sample produced in this work. However, the EDX analysis for the sample with nano Al_2O_3 with x=0.6 wt. % shows the existence of the Al element as shown in Fig. (1). As seen from these Figures, no differences appear between the samples produced except for Al peak, revealing that the Al is incorporated into the crystalline structure of the samples. Besides, the elements used for the preparation of samples are observed to distribute homogeneously. The result demonstrated there is no contaminations are observed in the spectra, which verify the high purity of the investigated samples.

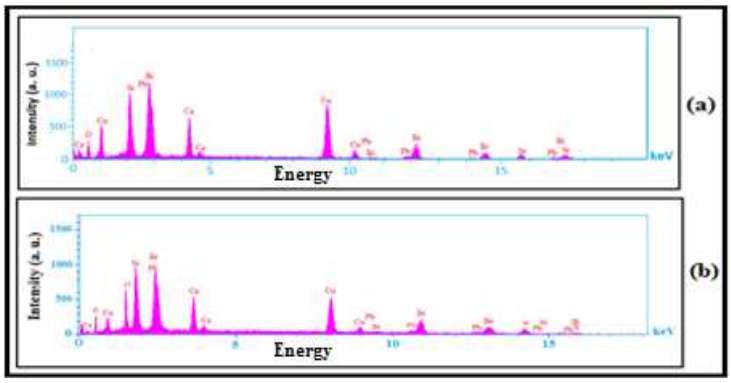

Fig.1: EDX Spectra of $(Al_2O_3)_0\ Bi_{1.7}\ Pb_{0.3}\ Sr_2\ Ca_2\ Cu_3\ O_{10+\delta}$ sample with (a) x=0.0 and (b) x= 0.6 wt. %.

X-Ray Diffraction:

XRD patterns of samples $(Al_2O_3)_x$ $Bi_{1.7}Pb_{0.3}Sr_2Ca_2Cu_3O_{10+\delta}$ superconductor ceramics produced in this work with x=0.0, 0.2, 0.4, and 0.6 wt.% nanoparticles addition are shown in Fig. (2).As can be seen from the figure, all the samples studied exhibit the polycrystalline superconducting phase with two phases, low T_c phase Bi-2212 and high T_c phase Bi-2223 phases. A weak impurity phase such as Ca_2PbO_4 peak at 2θ=32^{o}and other unknown impurities are identified in samples.

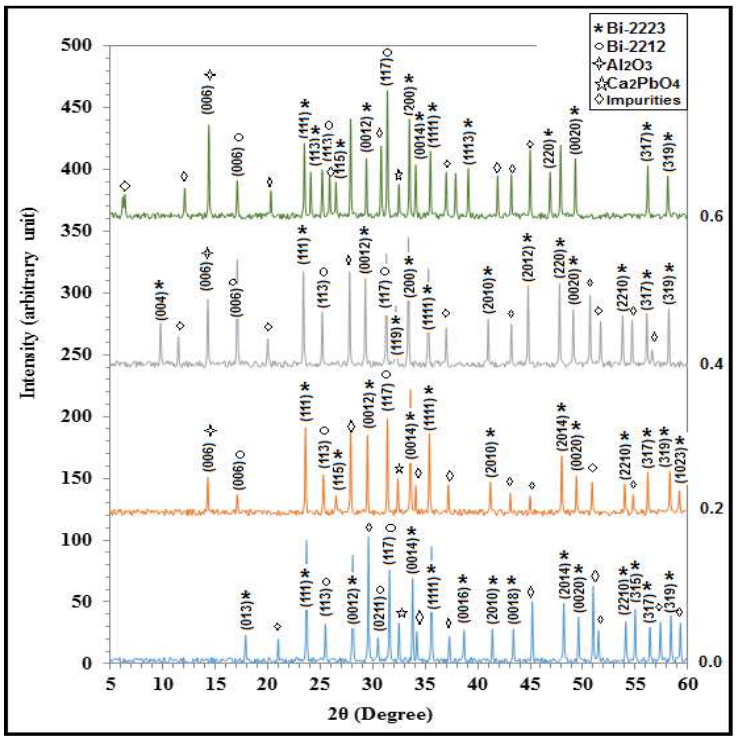

Fig.2: X-ray diffraction patterns for ($Bi_{1.7}$ $Pb_{0.3}$ Sr_2 Ca_2 $Cu_3O_{10+\delta}$) sample and sintered at 830°C for 140 h that added with nano γ (Al_2O_3).

The XRD patterns revealed that all the samples with (x=0.0, 0.2, 0.4, and 0.6) wt. % consist of Al_2O_3 peak at 2θ=14.3 for (006) Miller indisies this indicate that incorptionAl_2O_3 in the sample as conformed in EDS. The volume fraction of the present phase, high phase Bi-2223 and low phase Bi-2212 were determined used the following formulas (Abou-Aly, A.I., 2011).

$$B_i(2223)\% = \frac{\sum I(2223)}{\sum I(2223)+\sum I(2212)} * 100 \quad \text{.....(1)}$$

$$B_i(2212)\% = \frac{\sum I(2212)}{\sum I(2223)+\sum I(2212)} * 100 \quad \text{.....(2)}$$

Where I (2223) and I (2212) are the intensities of the (hkl) XRD peak for Bi-2223 and Bi-2212 respectively the calculated relative portions of each phase of the samples are listed in Table (1). One can see from the Table, the percentage of Bi-2223 phase decreases and the Bi-2212 phase increases with increasing the amount of the Al_2O_3 nanoparticles addition into our samples. In addition, the percentage of the high phases Bi-2223 have a high value for the sample with x=0.2 wt. % and did not change that much in comparing to sample with x=0.0 (Al_2O_3 – free sample). So it can be said that adding 0.2 wt. % Al_2O_3 nanoparticle to the BSCCO system almost did not reduce the amount of Bi-2223 phase. The percent amounts of the Bi-2223 and Bi-2212 as a function of x evaluated from the XRD patterns of (Al_2O_3) $Bi_{1.7}Pb_{0.3}Sr_2Ca_2Cu_3O_{10+\delta}$ sample are given in Fig. (2).Moreover, the lattice parameters a, b, and c are calculated using the least square method through d value and (hkl) planes for orthorhombic unit cell structure and depicted in Table (1). From this Table we see that the same lattice parameters were obtained for Al_2O_3 nanoparticles added samples. There is no distortion in the crystal system of the Al_2O_3 added Bi-2223, which shows that Al_2O_3 particles do not participate in the crystal structure of the Bi-2223. There for, we expected that the added of nanoparticles Al_2O_3 are sited between the superconducting grains andeither the role of such nanoparticle impurities can act as the pinning centers to fix vortices or they may enhance connectivity among the grains, which leads to higher J_c(Ghazanfaria, N., 2007).

Increasing of the intensities for all peaks up x=0.2, and these peaks were lower with increase of Al_2O_3 concentration can see in Fig. (2). On the other side a present of (00$\underline{12}$) at 2θ = 29.3 for all concentration of Al_2O_3 is very important to prove the superconductivity for Bi-2223 compound (Hermiz, G.Y., 2014). A weak impurity phase Ca_2PO_4 peak at 2θ=32° was identified in the shape ☆.And the peak important appear in 2θ=14.3° for Al_2O_3 was identified in the shape ✧, all these peak shown in Fig. (2).

It is shown from the Table (1) and Fig. (3b) that the c/a decreases slightly with increasing the concentration of Al_2O_3 nano particles concentration. The variation of lattice parameters a, b, c effect on the volume of the unit cell and change with concentration of Al_2O_3 also shown in Fig. (3b).

Electrical Resistivity Measurements:

Measurements of the resistivity dependence of temperature for different samples with various amount of nanoparticle addition of Al_2O_3 to the $Bi_{1.7}Pb_{0.3}Sr_2Ca_2Cu_3O_{10+\delta}$ are shown in Fig. (6). One can see from these figures all samples show metallic behavior in the normal state (dp/dt) and as superconducting transition to zero resistance, except samples with x= 0.8 and 1 wt.% which showed a semiconductor behavior. At high temperature (from room temperature) the normal state resistivity for all samples is found to be linear temperature dependence. At the temperature value T_c the electrical resistivity vanishes as seen in Fig. (5), the critical transition temperature T_c of the samples are obtain from the Fig. (6), and shown in Table (1). Based on the result, the T_c value is found to decrease with the increase of the Al_2O_3 nanoparticle addition as shown in Fig. (5), the high value of T_c was obtained for the sample with x= 0.2 wt. %. Also, for this amount of Al_2O_3 the transition to T_c seems to be a one-step transition (nearly sharp), indicating the formation of nearly Bi-2223 single phase. This is in agreement with XRD result which showed an increase in the Volume fraction of the prepared sample with x=0.2 wt. %. In this regard, small amount of sub nano sized particle addition improved flux pinning by creating effective pinning centers, while excessive Al_2O_3 doping degraded the superconducting of the BSCCO system. The depression of T_c with Al_2O_3 addition may be either due to a decrease in oxygen content in CuO chains or due to trap of mobile holes or some mechanism connected with oxygen vacant disorder. The higher concentration of nanoparticles supports the cooper pair breaking mechanism (Terzioglu, C., 2005). A similar result was observed by Aljurani et.al. (2015), in studying the effect of SnO_2 nanoparticles addition on (Bi, Pb)-2223 phase.

Table 1: Variation in lattice parameters, c/a, density of unit cell (ρ_m) and volume fraction of Bi-2223 and Bi-2212, for (Al_2O_3) ($Bi_{1.7}$ $Pb_{0.3}$ Sr_2 Ca_2 Cu_3 $O_{10+\delta}$) system

X wt.%	a Å	b Å	c Å	c/a	VÅ^3	VBi-2223 %	VBi-2212 %	T_c (K)
0	5.412	5.368	37.229	6.878	1081.563	83.879	16.121	110
0.2	5.430	5.356	37.239	6.858	1083.025	81.148	18.851	118
0.4	5.421	5.384	37.152	6.843	1082.825	77.700	22.300	113
0.6	5.439	5.338	37.031	6.808	1075.106	76.627	23.372	108

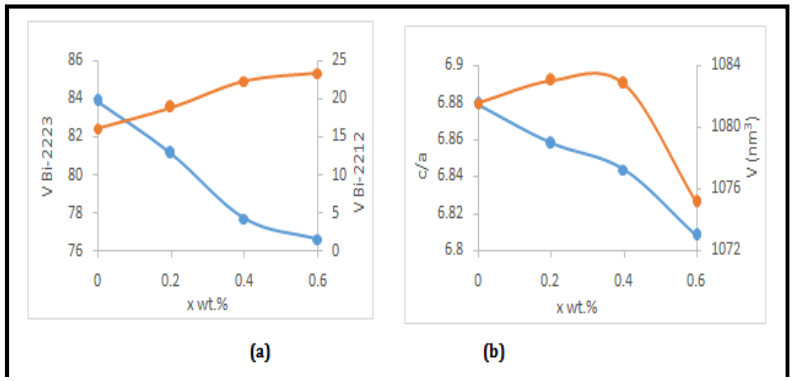

Fig.3:(a)Variation of Volume fraction forBi-2223 and Volume fraction for Bi-2212(b) Variation c/a and Volume (V) of unit cell as a function of Al_2O_3 nano concentration of $(Al_2O_3)_x$ ($Bi_{1.7}$ $Pb_{0.3}$ Sr_2 Ca_2 Cu_3 $O_{10+\delta}$) sample.

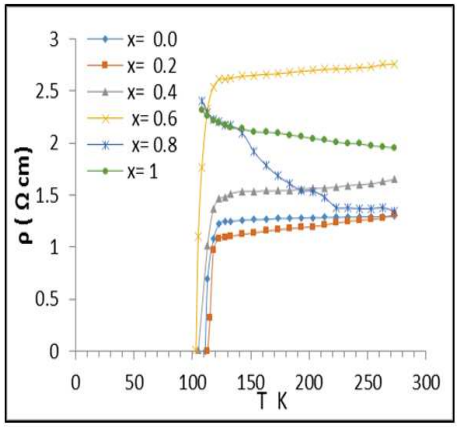

Fig.4: Resistivity (ρ) as a function of a temperature for $(Al_2O_3)_x$($Bi_{1.7}$ $Pb_{0.3}$ Sr_2 Ca_2 Cu_3 $O_{10+\delta}$).samples for different concentration of nano (Al_2O_3).

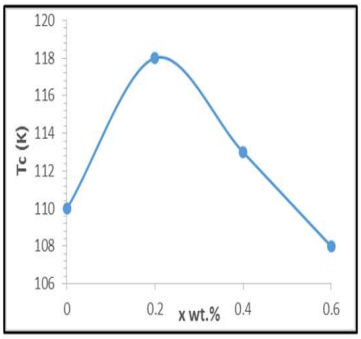

Fig.5: Variation of T_c with γ Al_2O_3 nano particles addition concentration (x) for $(Al_2O_3)_x(Bi_{1.7}\,Pb_{0.3}\,Sr_2\,Ca_2\,Cu_3\,O_{10+\delta})$.

SEM Analyses:

The images of surface morphology of the samples $(Al_2O_3)_x$ $Bi_{1.7}Pb_{0.3}Sr_2Ca_2Cu_3O_{10+\delta}$ are performed by Scanning Electron Microscope (SEM). Figure (6 a-d) indicates the SEM images of the fractured surface of the superconducting samples prepared with different concentration of Al_2O_3 nanoparticles with x=0.0, 0.2, 0.4, and 0.6 wt. % respectively. It is clearly seen from the Figure that the surface morphology changes with addition of nanoparticles Al_2O_3 atoms in the (Bi, Pb)-2223 system. The grain morphology of the pure sample nanoparticles free Fig. (8-a) show a large plate-like structure with random alignment distribution. Moreover, the texturing and layered grain growth are observed for the samples added with (Al_2O_3) nanoparticles x=0.2 as shown in Fig. (6-b),the increase in the size of whisker (plate- like structure) at this concentration of Al_2O_3 lead to decrease the number of porosity. These particles can enhance the connectivity among the grains and they can increase the pinning centers of fix the vortices. The SEM results corroborate well with the XRD results. A decrease in the grain size is observed for samples c and d that may reduce superconducting properties of the BSCCO system. This indicates that the concentration of nanoparticles Al_2O_3 above x=0.2 act as a barrier and hinder the grains growth.

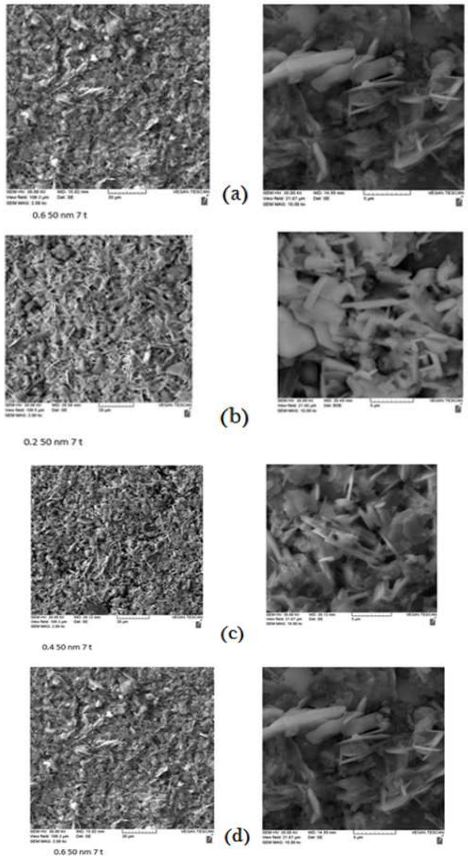

Fig.6:SEM patterns of $(Al_2O_3)_x$ (a=0.0) (b=0.2) (c=0.4) and (d=0.6) wt.% for $(Al_2O_3)_{x\ x}(Bi_{1.7}\,Pb_{0.3}\,Sr_2\,Ca_2\,Cu_3\,O_{10+\delta})$ samples.

Australian Journal of Basic and Applied Sciences, 9(35) November 2015, Pages: 54-60

Atomic Force Microscope (AFM) Analysis:

AFM measurement was performed in order to obtain surface to prographic images of the samples and was used to monitor the morphological change of Al_2O_3 nanoparticle addition in Bi-2223 samples. The surface nature of the samples were analyzed with regard to different composition $(Al_2O_3)_xBi_{1.7}Pb_{0.3}Sr_2Ca_2Cu_3O_{10+\delta}$ with $(0\leq x\leq 0.6)$. Fig. (7 a-d) show Two-diminution (2D). AFM image of samples revealed the nano granular structure on the surface. A systematic scanning analysis was carried out at different location of samples (pellets) with different resolution, and magnification. The images demonstrate that the samples are homogeneous and uniform. Also, the morphology contains well (defined) and highly aligned plate-like grains on all sides of its growth front.

In the three deamination (3D) Fig. (8 a-d) show. AFM images of the same surface. The formation of humps and roughness in same places could also be clearly seen, which is due to formation of superconducting layer with different thickness depending on the chemical composition of phases (Aljurani, B., M. Aldulaimi, 2015). These images were used to estimate the mean size of nanoparticles. It can be observed that the average size of the nanoparticles are about (112 – 90 nm). The value of particle size and Al_2O_3 concentration of Bi-2223 are shown in Table (2). The graphs of particle size and Al_2O_3 concentration of Bi-2223 are shown in Fig. (9). Also, the AFM was used to measure the root mean square roughness of Al_2O_3 nanoparticles addition of Bi-2223 sample. Surface roughness is calculate as the standard deviation of the mean high of surface structure. It is observed from Table (2) that the roughness of the sample increased with increasing Al_2O_3 concentration.

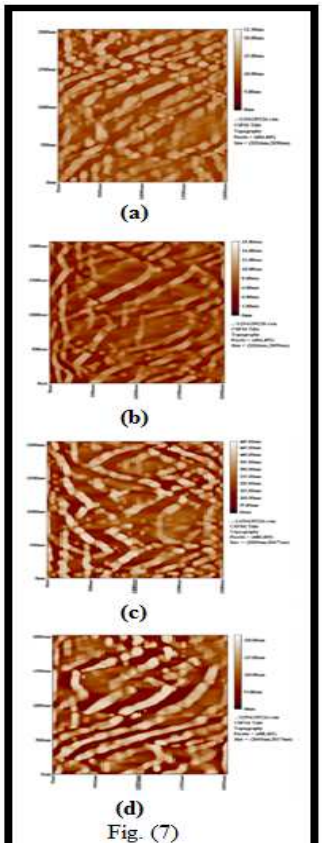

Fig. (7)

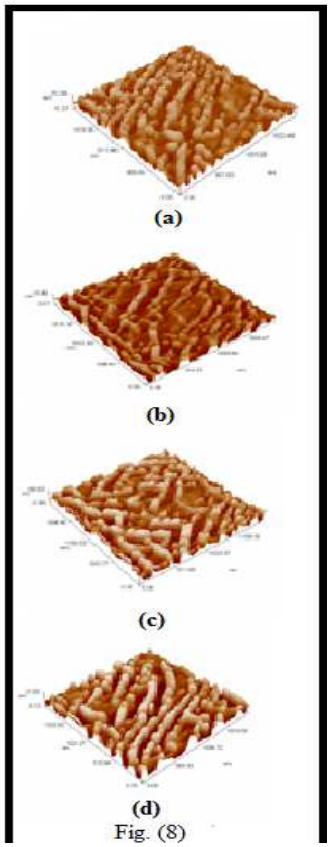

Fig. (8)

Fig.7: AFM (2D) patterns of $(Al_2O_3)_x$ (a=0.0) (b=0.2) and (c=0.4) and (d=0.6) wt.% for $(Al_2O_3)_x$ $(Bi_{1.7}\,Pb_{0.3}\,Sr_2\,Ca_2\,Cu_3\,O_{10+\delta})$ samples.

Fig.8: AFM (3D) patterns of $(Al_2O_3)_x$ (a=0.0) (b=0.2) and (c=0.4) and (d=0.6) wt.% for $(Al_2O_3)_x$ $(Bi_{1.7}\,Pb_{0.3}\,Sr_2\,Ca_2\,Cu_3\,O_{10+\delta})$ samples.

Table 2: Variation Roughness (Sa), Root mean saqure (Sq), and Average particle size for different concentration (x) of $(Al_2O_3)_x(Bi_{1.7}\,Pb_{0.3}\,Sr_2\,Ca_2\,Cu_3\,O_{10+\delta})$ system.

γAl_2O_3	X wt. %	Sa nm	Sq nm	Average particle size (nm)
50 nm	0.0	2.51	2.88	112.15
	0.2	1.84	2.14	90.39
	0.4	8.10	9.33	94.79
	0.6	12.19	14.81	96.01

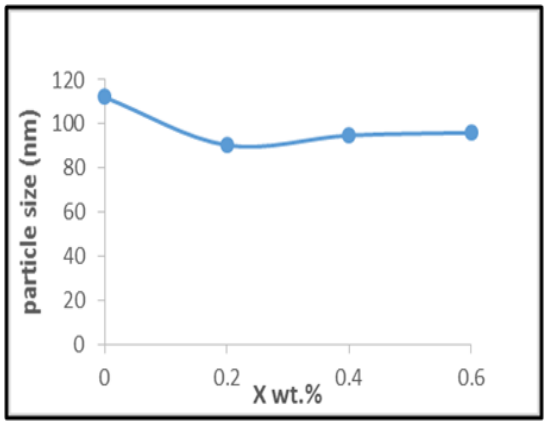

Fig.9: Variation particle size as a function of γ Al_2O_3 nano concentration of $(Al_2O_3)_x$ ($Bi_{1.7}$ $Pb_{0.3}$ Sr_2 Ca_2 Cu_3 $O_{10+\delta}$) sample.

Conclusion:

It was found that the addition of γAl_2O_3 nano-particle to (Bi-Pb)-2223 superconducting phase increased the volume fraction, and the superconducting transition temperature. The higher concentrations of Al_2O_3 nano-particles x>0.2 wt. % reduced phase formation and superconducting transition temperature of (Bi, Pb)-2223. This was attributed that high concentration of Al_2O_3 nano-particle, induced large agglomeration between superconducting grain connectivity and deteriorated of intergranular current density.

REFERENCES

Abd Shukor, R., 2004. "Introduction to superconductivity in Metals, Alloys, and Cuprates" First Printing, PenerbitUniversiti Sultan Idris TanjongMalim, (1).

Maeda, H., Y. Tanaka, M. Fukutomi and T. Asano, 1988. "A New High-T_c Oxide Superconductor without a Rare Earth Element". Jpn. J. Appl. Phys.part, 2(27): L209.

Michel, C., M. Hervieu, M.M. Borel, A. Grandin, F. Deslandes, J. Provost, B. Raveau, 1987. "Superconducting in the Bi-Sr-Cu-O system." Z phys B., 68(4): 421-3.

Rentschler, T., Kemmler,S. Sack, M. Hartmann, HubenenRp, P. Kesselar, H. Lichte, 1992. "Influence of Nd substitution on the superconducting properties of ceramics in the 2212 system $Bi_{2-w}Pb_wSr_{2-y}Nd_{x+y}Cu_xO_{8+\delta}$, Phys C supercond, 200(3-4): 287-95.

Hermiz, G.Y., B.A. Aljurani, H. Al-Beayty Md. Ali, 2014. "Effect of substitution on the superconducting properties 0f $Bi_{1.7}Pb_{0.3}Sr_2Ca_{2-x}Mn_xCu_3O_{10+\delta}$. International Journal of Enginering and Advanced Technology (IJEAT),2249-8958, 3-4.

Yildirim, S., E. Ral, M. Yucel, M. Dogruer, A. Akdogan, C. Varilci, TerZioglu, 2012. "Effect of Mn addition on structural and superconducting properties of (Bi,Pb)-2223 superconducting Ceramics" J supercond Nov Magn, 25: 381-390.

Zelati, A., A. Amirabadizadeh, A. Kompany, H. Salamte, J. Sonier, 2014. "Effects of Dy_2O_3 nanoparticle addition on structural and superconducting properties of BSCCO".Indian Journal of Science and Technology 7(2): 123-134.

Hamid, N.A., 2009. "Effect of TiO_2 addition on superconducting properties of BSCCO system". Journal of material science, 35: 2325-2329.

Baqiah, H., Halim, S.A. Adam, M.I. Chen, S.K. Ravandi, S.S.H. Faisal, M.A.M. Kamarulzaman, M.M. Hanif, 2009. "Solid State Sci. Technol", 17-81.

Jannah, A.N.R., Abd-Shukor and H. Abdullah, 2013. "Word Academy of science and Technology", 75: 367.

Abou-Aly, A.I.,M.M.H. Abdel gawad, R. Awad and I.R. G-Eldeen, 2011. "Improving the physical properties of (Bi, Pb)-2223 phase by SnO2 nano-particles addition", journal of superconductivity and Novel Magnetism, 24: 2077.

Ghazanfaria, N., A. Kilic, A. Gencerb, H. Ozkana, 2007. "Effect of Nb_2O_5 addition on superconducting properties of BSCCO" Solid State Comm., 144(5-6): 210-4.

Barik, H.K., S.K. Ghorai, S. Bhattacharya, D. Kilian, B.K. Chaudhuri, 2000. J. Mater. Res. 15, 1076.

Terzioglu, C., M. Yilmazlar, O. Ozturk, E. Yanmaz, 2005. Physica C., 423-119.

Aljurani, B., M. Aldulaimi, 2015. "Improvement of superconducting properties of of (Bi, Pb)-2223 added with nano-particales SnO_2" International Journal of Current Engineering and Technology (IJCET), 5(2).

Kumar, R., InduVerma, Nidhi Verma, V. Ganesan, 2012. "Effect of Mn on the Surface Morphological Properties of $(Bi, Pb)_2$ $Sr_2Ca_2Cu_{3-x}Mn_xO_{10+\delta}$ (Bi-2223) superconductor" J supercond Nov Magn, 25: 1215-1221.